Geometry of Separation Boundaries: Systems with Reaction

ARTICLE *in* INDUSTRIAL & ENGINEERING CHEMISTRY RESEARCH · MARCH 2006

Impact Factor: 2.59 · DOI: 10.1021/ie0508740

3 AUTHORS, INCLUDING:

Angelo Lucia
University of Rhode Island
102 PUBLICATIONS **809** CITATIONS

SEE PROFILE

SEPARATIONS

Geometry of Separation Boundaries: Systems with Reaction

Ross Taylor* and Amanda Miller

Department of Chemical and Biomolecular Engineering, Clarkson University, Potsdam, New York 13699

Angelo Lucia

Department of Chemical Engineering, University of Rhode Island, Kingston, Rhode Island 02881

Residue curves and residue curve maps have been extensively studied for over 100 years. Much of the literature in this field deals with systems that do not react. Chemical reactions can influence residue curve maps in some important ways. For example, it is known that reactions can lead to both the appearance and disappearance of stationary points (azeotropes), and that reactive azeotropes can exist even in systems that otherwise would be considered thermodynamically ideal. It follows that chemical reactions can influence the very existence of separation boundaries and, therefore, the design and synthesis of reactive separation processes. Lucia and Taylor (*AIChE J.* **2006**, *52*, 582) have shown that distillation boundaries in nonreacting ternary liquid mixtures can be defined as local maxima in the line integral from any unstable node to all reachable stable nodes. This paper shows how this geometric approach can be adapted for the rigorous determination of separation boundaries in reacting mixtures. Evidence is provided to show that boundaries in systems with two degrees of freedom are maximum line integrals. Examples of such systems include four-component systems with a single equilibrium reaction and ternary systems with a kinetically controlled reaction.

Introduction

Residue curves and residue curve maps have been extensively studied for over 100 years, beginning with the work of Ostwald[2,3] and Schreinemakers.[4] For mixtures that have azeotropes, separation boundaries may exist, and these boundaries are important in separation process synthesis (see, for example, ref 5).

Much of the literature in this field deals with systems that do not react. However, over the last 20 years or so, reactive separations have come in for considerable attention (see, for example, Chapter 10 of ref 5 and ref 6). Chemical reactions can influence residue curve maps in some important ways. For example, reactions can lead to the disappearance of some azeotropes that exist in the absence of reaction. Chemical reactions can also lead to the creation of new azeotropes that would *not* exist in the absence of reaction. Moreover, it is possible for these so-called reactive azeotropes to exist even in systems that otherwise would be considered thermodynamically ideal. It follows that chemical reactions can influence the very existence of separation boundaries and, therefore, the design and synthesis of reactive separation processes.[5]

For nonreacting ternary systems, separation boundaries may be characterized in terms of line integrals, surface areas for four-component systems, volumes for five-component systems, and so on. In particular, Lucia and Taylor[1] show that separation boundaries for ternary azeotropic nonreacting liquid mixtures can be characterized as local maxima in the line integral from any unstable node to all reachable stable nodes. This property of separation boundaries allows us to use an optimization method to precisely locate these boundaries.

It is the purpose of this paper to show how the geometric approach described by Lucia and Taylor[1] can be adapted for the rigorous determination of separation boundaries in reacting mixtures. Toward this end, we continue with a brief introduction to the key concepts from the approach of Lucia and Taylor[1] to defining and computing distillation boundaries in nonreacting systems. In subsequent sections, we look at the residue curve maps for mixtures in chemical reaction equilibrium before turning our attention to kinetically limited reacting mixtures. Finally, we provide a summary of our conclusions.

Residue Curve Maps for Nonreacting Systems

The simple distillation of a liquid mixture is modeled by

$$\frac{dx_i}{d\xi} = x_i - y_i \tag{1}$$

where ξ is a dimensionless time, x_i is the mole fraction of species i in the liquid phase, and y_i is the mole fraction of species i in the vapor phase. The liquid- and vapor-phase mole fractions are related through the familiar equations of phase equilibrium,

$$y_i = K_i x_i; \quad \sum_{i=1}^{c} (y_i - x_i) = 0 \tag{2}$$

where K_i is the equilibrium ratio or K-value for species i.

These are the equations that describe residue curves in nonreacting systems, and they have been very extensively

* To whom correspondence concerning this article should be addressed. Tel.: (315) 268-6652. Fax: (315) 268-6654. E-mail: taylor@clarkson.edu.

10.1021/ie0508740 CCC: $33.50
Published on Web 03/17/2006

studied (for reviews of the literature, see refs 5 and 7−10). The (numerical) solution of these equations provides a family of curves known as a residue curve map.

The stationary points of eq 1 are the pure-component vertices and azeotropic points, and these fixed points are repelling (unstable nodes), attracting (stable nodes), or both (saddle points). The connections between these points, known as distillation boundaries, divide composition space into distinct regions (see, for example, ref 5, p 195). The location of these boundaries has an important bearing on separation process synthesis. It is often preferable to design a process to stay away from a boundary. However, in some cases, these boundaries are strongly curved and approximate methods of locating such boundaries may not be sufficiently precise for design purposes. Kiva et al.[10] are careful to distinguish between exact and approximate boundaries; the former can be determined only by repeated integration of eq 1. However, even repeated integration in the absence of a systematic method of locating the boundaries may not suffice; we have found cases where as many as 1000 integrations of eq 1, starting from the near neighborhood of a stationary point, will fail to locate the boundary even approximately. What was missing was a precise definition of a boundary that could be used as the formal basis for a systematic procedure for locating boundaries.

Geometric Methodology of Separation Boundaries. Lucia and Taylor[1] define a separation boundary for any ternary mixture as the trajectory (or integral curve), say $x^*(\alpha)$, associated with the solution of the nonlinear programming problem

$$\max_{x(0)} D = \int_0^T ||x'(\alpha)||\, d\alpha \tag{3}$$

subject to

$$x'(\alpha) = x(\alpha) - y[x(\alpha)]; \quad x(T) = x_T \tag{4}$$

where D represents a line integral or distance function along a trajectory, $||\cdot||$ denotes the two-norm, $x(0)$ is any feasible set of initial conditions on the ball (or circle in the case of a ternary mixture) of radius ϵ about some designated unstable node $\mathbf{x}_0$, and x_T is a stable node. The ball of radius ϵ about a designated unstable node $\mathbf{x}_0$, is defined by $B(\mathbf{x}_0,\epsilon) = \{\mathbf{x}: ||\mathbf{x} - \mathbf{x}_0|| = \epsilon$ for all $\mathbf{x}\}$, and it is important to note that the objective function, D, in eq 3 is only a function of the initial conditions, $\mathbf{x}(0)$, which are the unknown optimization variables. Thus, any trajectory, $\mathbf{x}^*(\alpha)$, that corresponds to a local maximum value of the line integral is a separation boundary.

Note that, as shown in subsequent examples, the trajectory, $\mathbf{x}^*(\alpha)$, can pass directly through a saddle point node and then split or bifurcate and continue to two different stable nodes. Lucia and Taylor also show that their approach readily extends to more components by replacing the line integral in eq 3 by surface areas and volumes for four- and five-component systems, respectively.

Example 1: Isobutene−Methanol−MTBE (Methyl *tert*-Butyl Ether). Figure 1 shows a residue curve map for the ternary nonreacting mixture isobutene (1)−methanol (2)−MTBE (3) at a pressure of 11 atm. We have included this system because it is widely used in the literature on reactive distillation (see, for example, ref 5), and we shall consider this example again later in the paper. The arrows on the residue curves in Figure 1 show the direction of flow, in this case from low temperature to high (as is frequently, but not universally, done). This system has two binary azeotropes; with regard to eq 1, the isobutene−methanol azeotrope is an unstable node and the

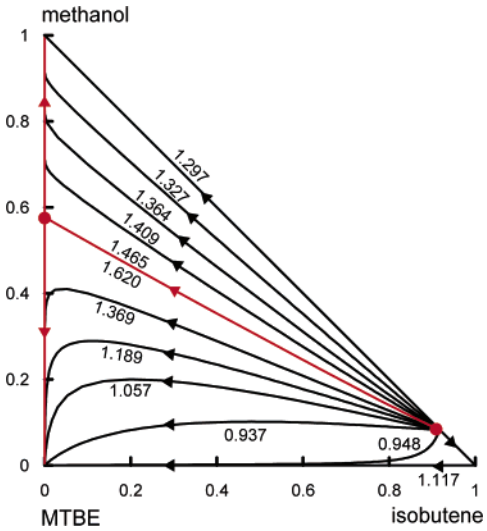

Figure 1. Residue curves in the nonreacting ternary system isobutene−methanol−MTBE at 11 atm. Numbers near residue curves are the lengths of the corresponding curve: ●, azeotrope.

methanol−MTBE binary azeotrope is a saddle point. In addition, the isobutene vertex is a saddle point, and the MTBE and isobutene vertices are stable nodes.

There is a separation boundary that divides the composition triangle into two parts along a line that appears to run from the isobutene−methanol azeotrope to the methanol−MTBE saddle point. All residue curves in Figure 1 that lie above this boundary go between the isobutene−methanol azeotrope and the methanol vertex; the residue curves below the boundary end at the MTBE vertex. The separation boundary itself is, in theory, a single curve from the isobutene−methanol azeotrope that subsequently splits and goes to both the pure methanol and pure MTBE vertices. In practice, however, the portion of the separation boundary that runs from the isobutene−methanol azeotrope vertex to the methanol−MTBE azeotrope will actually be two distinct but essentially coincident trajectories that turn away from each other very close to the methanol−MTBE azeotrope. We suggest that it is essential to view a boundary as an integral curve that runs from an unstable node to a stable node. It is only from this perspective that separation boundaries correspond to local maxima in line integrals for ternary mixtures.

Figure 2 shows the behavior of $D(\theta)$. To create this diagram, we computed residue curves for 1000 points equally spaced in the interval $3\pi/4 \le \theta \le 7\pi/4$ around the point isobutene−methanol azeotrope (on the hypotenuse of the triangle in Figure 1) with a radius $\epsilon = 0.001$. There is one discontinuity in $D(\theta)$ corresponding to the boundary described above. This discontinuity (and, perforce, the boundary) can be found quite straightforwardly using the optimization method devised by Lucia and Taylor.[1] The minimum in Figure 2 corresponds to the shortest residue curve in this system, from the isobutene−methanol azeotrope to the MTBE vertex.

Equilibrium Reactions

The effect that equilibrium chemical reactions have on residue curves in two-phase (vapor−liquid) systems has been considered at length by Doherty and co-workers.[11−20] In their first paper, Barbosa and Doherty[11] look at the influence of a single reversible chemical reaction on vapor−liquid equilibria. Their second paper[12] introduces a set of transformed composition variables that are particularly useful in the construction of thermodynamic diagrams for reacting mixtures. For a system

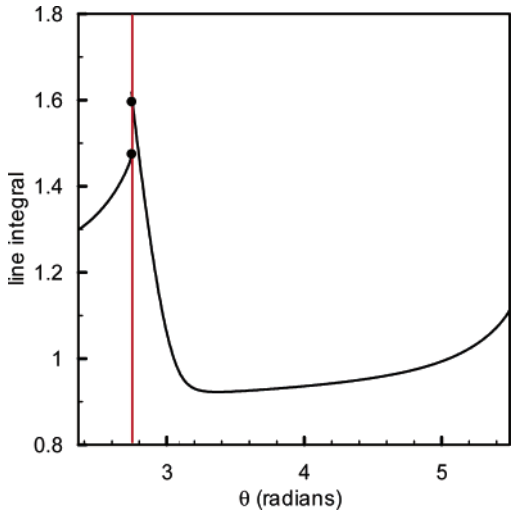

Figure 2. Line integral as a function of departure angle from the isobutene−methanol azeotrope for the nonreacting ternary system isobutene−methanol−MTBE: ● , maximum line length.

in which the components take part in either of the following reactions,

$$A + B \leftrightarrow C$$

$$A + B \leftrightarrow C + D$$

the following transformation is defined

$$Z_i = \frac{z_i - \nu_i z_k}{1 - \nu z_k} \tag{5}$$

where Z is the transformed composition ($Z \in \{X,Y\}$) and z is the corresponding mole fraction ($z \in \{x,y\}$). The subscript k refers to a reference component (for the selection of which Barbosa and Doherty provide some guidelines). The number of independent transformed composition variables is $c - r - 1$, where c is the number of components and r is the number of independent reactions. Barbosa and Doherty[13] provide a method for the construction of phase diagrams of reactive mixtures, while Doherty[15] develops the topological constraints for residue curve maps of four-component systems. Ung and Doherty[16−20] have extended the methods of Barbosa and Doherty to deal with mixtures with arbitrary numbers of components and reactions.

In terms of the transformed composition variables, the material balance equations that describe a simple open evaporation in a reacting mixture are given by

$$\frac{dX_i}{d\xi} = X_i - Y_i \tag{6}$$

where X_i is the transformed composition of species i in the liquid phase and Y_i is the transformed composition for the vapor phase. ξ is a dimensionless time. The residue curves for a system in reaction equilibrium are obtained from a numerical solution of the differential equations (eq 6), two sets of equations (eq 5) relating the transformed composition variables to the mole fractions, the phase-equilibrium equations (eq 2), and the equations for reaction equilibrium, which, for a single liquid-phase reaction, can be written as

$$K_R = \prod_{i=1}^{c} (\gamma_i x_i)^{\nu_i} \tag{7}$$

In eq 7, K_R is the reaction equilibrium constant, and the stoichiometric coefficients, ν_i, are positively signed for products, negative for reactants, and zero for inert compounds.

According to Rowlinson,[21] "A system is azeotropic when it can be distilled (or condensed) without change of composition". The conditions for the existence of azeotropes in reacting systems are most easily expressed in terms of the transformed composition variables[12]

$$X_i - Y_i = 0 \tag{8}$$

The points $X_i = Y_i$ are the stationary points of eq 6. Note that, in contrast to the situation that holds for systems that do not react, not all of the pure components and azeotropes of the equivalent nonreacting system are solutions of eq 8 (for example, it is not possible for reaction products to exist as pure components in the presence of an equilibrium reaction). Thus, reactions can cause the disappearance of some azeotropes that exist in the absence of reaction. Chemical reactions can lead to new (reactive) azeotropes that also would *not* exist in the absence of reaction. It is possible for reactive azeotropes to exist even in systems that otherwise would be considered thermodynamically ideal.[11,12] Reactive azeotropes have been found for the system 2-propanol−isopropyl acetate−water−acetic acid (ref 22) and propyl acetate (ref 23). The influence that the reaction equilibrium constant has on the existence and location of reactive azeotropes has been investigated for single-reaction systems by Okasinski and Doherty.[24] Maier et al.[25] have proposed a method based on interval analysis for finding all solutions to eq 8.

As is true for nonreacting systems, the stationary points defined by eq 8 are stable nodes, unstable nodes, or saddle points. The connections between these points form part of any boundaries that divide transformed composition space. Thus, reactions influence the very existence of simple separation boundaries in reacting systems.

Geometric Methodology of Separation Boundaries in Equilibrium Reacting Systems. It is clear that the equations describing the simple distillation of equilibrium reacting mixtures retain the form and underlying dynamical behavior of the eq 1 for nonreacting systems. This suggests that the geometric approach described by Lucia and Taylor[1] can be adapted for the rigorous determination of separation boundaries in reacting mixtures. We conjecture that local maxima in line integrals, surface areas, volumes, and so on in the space defined by the transformed compositions in eq 5 define separation boundaries for mixtures in reaction equilibrium. Thus, for a system with two degrees of freedom (four components with one equilibrium reaction, five components with two equilibrium reactions, etc.), the boundary may be defined by

$$\max_{X(0)} D = \int_0^T ||X'(\alpha)||\, d\alpha \tag{9}$$

subject to

$$X'(\alpha) = X(\alpha) - Y(\alpha); \quad X(T) = X_T \tag{10}$$

Lucia and Taylor[1] present in detail a feasible path-optimization method for solving the problem defined by eqs 9 and 10.

Example 2: Ideal Four-Component System. Consider the hypothetical system studied by Barbosa and Doherty[13,14] that reacts as follows:

$$A + B \rightleftarrows C + D$$

Phase equilibrium for this hypothetical ideal system is represented by a simple relative volatility model:

$$y_B x_A = \alpha_{B,A} x_B y_A; \quad y_C x_A = \alpha_{C,A} x_C y_A; \quad y_D x_A = \alpha_{D,A} x_D y_A \tag{11}$$

Chemical reaction equilibrium in the liquid is represented by

$$K_R = \frac{x_C x_D}{x_A x_B} \tag{12}$$

The phase-equilibrium model is completed by the two mole fraction summation equations.

The reaction equilibrium and liquid-phase summation equations may be solved to give the liquid-phase composition as a function of any two liquid-phase mole fractions; for example,

$$x_A = \frac{x_C(1 - x_B - x_C)}{x_C + K_R x_B}; \quad x_D = \frac{K_R x_B (1 - x_B - x_C)}{x_C + K_R x_B} \tag{13}$$

The vapor-phase mole fractions may then be obtained explicitly from the VLE equation (eq 11).

To compute the residue curves for a system like this with four components and one reaction, we need two of eq 6, eq 14 for the transformed composition variables, eq 11 for the VLE, and eq 12 for the reaction equilibrium (plus two mole fraction summation equations). Following Barbosa and Doherty,[13,14] we choose *D* to be the reference component. The transformed composition variables become

$$X_A = -x_A - x_E; \quad X_B = -x_B - x_E; \quad Y_A = -y_A - y_E; \quad Y_B = -y_B - y_E \tag{14}$$

We must also specify the values of the relative volatilities and the reaction equilibrium constant; here, these are assigned the following values: $\alpha_{B,A} = 1.7$, $\alpha_{C,A} = 3.9$, $\alpha_{D,A} = 4.2$, and $K_R = 0.76$. With these property values, the reactants A and B are the least volatile species in this system (and both are stable nodes) and the products C and D are the most volatile (and are unstable nodes).

For this relatively simple system, it is possible to express the transformed compositions for the vapor phase as explicit functions of X_A and X_B. Thus, the right-hand side of eq 6 can be expressed solely in terms of these variables (and the property constants). This makes the integration of these equations particularly straightforward, and for this system we used a simple Euler method (with a small step size).

Figure 3 displays the residue curves in terms of the transformed composition variables, and we can clearly see what looks like a saddle point azeotrope in what is a thermodynamically ideal system. The composition of the singular points for this system can, in fact, be found algebraically (because of the relative simplicity of the reaction and the phase-equilibrium equations). Simply by inspection we can see that the longest curves in Figure 3 are those that reach (almost to) the saddle point. There is a boundary located at a departure angle of approximately $\theta = 4.31$ rad, leaving the point $X_A = 0$, $X_B = 0$ (the D vertex) traveling by way of the reactive saddle-point azeotrope, where it splits into two branches, one which terminates at the A vertex and the other which terminates at the B vertex. The second boundary line can be found at a departure angle of approximately $\theta = 0.42$ rad, leaving the unstable node at $[-1, -1]$ (the C vertex) through the reactive saddle-point azeotrope to the stable nodes at A and B.

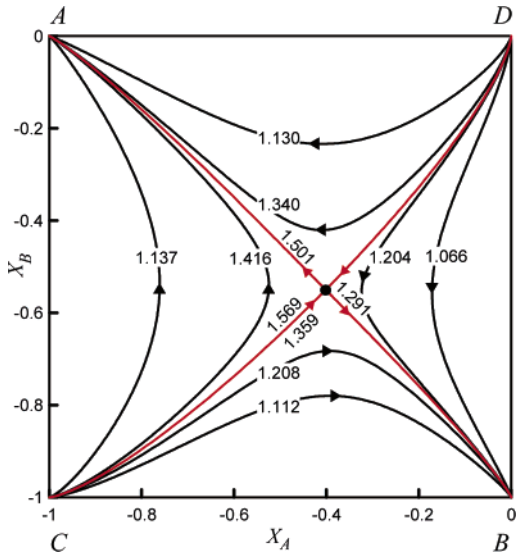

Figure 3. Residue curve map for reactive four-component ideal system: ●, azeotrope.

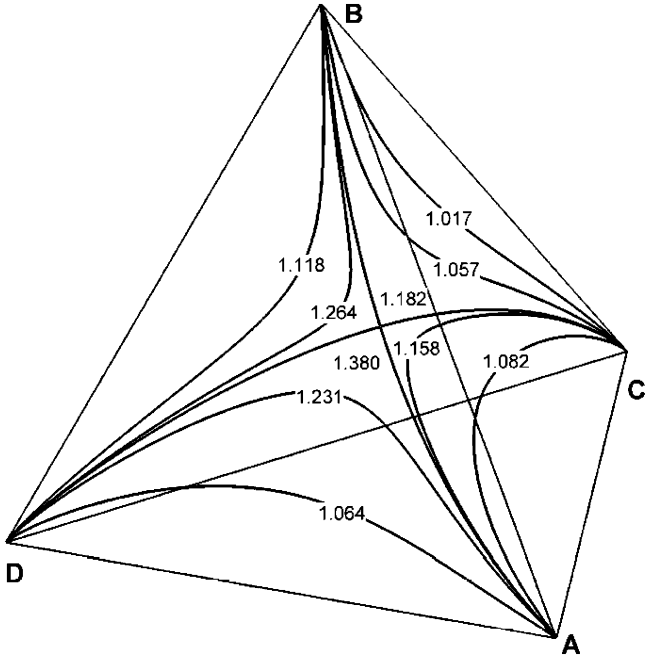

Figure 4. Residue curves for ideal system in mole fraction space. Numbers represent lengths of nearest residue curve in mole fraction space.

Figure 4 shows the residue curve map in mole fraction space; the numbers are the length of the closest residue curves in mole fraction space. It should be emphasized that the residue curves lie on the reaction equilibrium surface (as they must). Since the reaction equilibrium surface really is two-dimensional (although in some non-Euclidean geometry), it follows that the length of the boundary should also be a maximum line integral on this surface. Our calculations confirm that, indeed, the boundary is a maximum line integral in mole fraction space. The saddle-point azeotrope is clearly visible in Figure 4.

Example 3: Acetic Acid (1)/2-Propanol (2)/Isopropyl Acetate (3)/Water (4). When suitably catalyzed, a mixture of acetic acid and 2-propanol reacts to form isopropyl acetate and water:

$$\text{acetic acid} + \text{2-propanol} \rightleftarrows \text{isopropyl acetate} + \text{water}$$

This system has been investigated experimentally by Song et

al.[22] Venimadhavan et al.[26] present in detail the model used for vapor−liquid equilibrium in this four-component system,

$$y_i = \frac{P_{\text{sat},i}\gamma_i x_i}{\zeta_i P} \tag{15}$$

where $P_{i,\text{sat}}$ is the vapor pressure calculated from the Antoine equation and γ_i is the activity coefficient for which we used the NRTL model (parameters for these models are given in refs 25 and 26). ζ_i is a correction factor introduced to account for association of a component in the vapor phase. The correction for the associating species is

$$\zeta_A = \frac{1 + \sqrt{1 + 4kP_{\text{sat,A}}}}{1 + \sqrt{1 + 4Pky_A(2 - y_A)}} \tag{16}$$

and for the nonassociating species is

$$\zeta_N = \frac{2(1 - y_A + \sqrt{1 + 4Pky_A(2 - y_A)})}{(2 - y_A)(1 + \sqrt{1 + 4Pky_A(2 - y_A)})} \tag{17}$$

$\zeta_i = 1$ for all species when none of the components in the vapor phase associate. The subscripts A and N refer to the associating (only acetic acid here) and nonassociating (all other) species, respectively. k is the dimerization constant given by

$$\log k = -12.5454 + 3166/T \tag{18}$$

Reaction equilibrium for this case is represented by

$$K_R = \frac{\gamma_3 x_3 \gamma_4 x_4}{\gamma_1 x_1 \gamma_2 x_2} \tag{19}$$

Following Venimadhavan et al.,[26] we use $K_R = 8.7$. Note that eq 19 is solved numerically following rearrangement to a form that avoids division.

In the presence of reaction, the binary azeotrope between isopropyl acetate and water and the ternary azeotrope disappear, leaving the two other binary azeotropes. In addition, there is a reactive azeotrope involving all four components. We found the stationary points quite easily using Newton's method from a starting point obtained using a method described in Appendix A.

To compute the residue curves, we integrate eq 6 for the transformed compositions which here are given by

$$X_1 = x_1 + x_3; \quad X_2 = x_2 + x_3 \tag{20}$$

with similar relationships for the vapor phase. Isopropyl acetate was chosen to be the reference component. The method used to compute the residue curves is described in Appendix A.

A residue curve map (RCM) for this system in transformed composition space is shown in Figure 5. Notice that each of the vertices of the composition square corresponds to a pure component. All curves start at (more precisely, extremely close to) the reactive azeotrope that is an unstable node for this system. There are two boundaries that run from the reactive azeotrope to the surviving binary azeotropes on the 2-propanol−isopropyl acetate and 2-propanol−water axes and then to the appropriate pure-component nodes. The corresponding lengths of the residue curves on each side of the boundary are shown in Figure 5. We see that, as anticipated, the boundaries are the curves of maximum length.

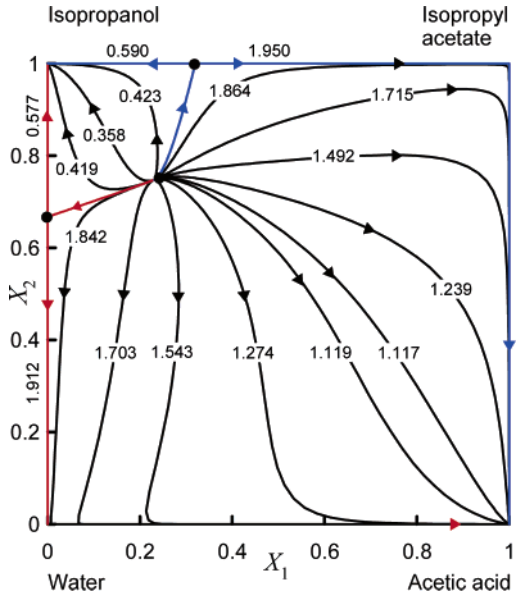

Figure 5. Residue curve map for isopropyl acetate chemistry at 1 atm. Numbers represent length in transformed composition space of corresponding residue curve: ● , azeotrope.

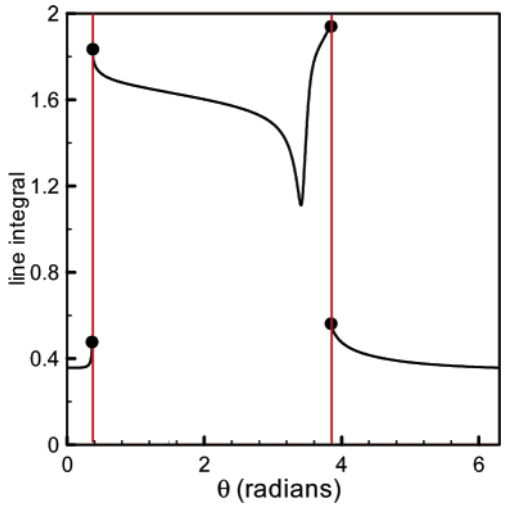

Figure 6. Line integral vs θ for acetic acid system: ● , maximum line length.

Figure 6 shows the line length in transformed composition space as a function of θ. To create this diagram, we computed residue curves for 1000 points equally spaced on a circle of radius $\epsilon = 0.01$ and centered on the reactive azeotrope (the only unstable node in this system). Use of a smaller radius is not recommended for this example because it will be difficult to locate the boundary with any precision (cf. Example 3 of Lucia and Taylor[1]). We see in Figure 6 the cusp-like discontinuities at the boundaries that now we should expect to see. The rather sharp minimum near $\theta = 3.4$ corresponds to the curve that takes the shortest path from the quaternary reactive azeotrope to the acetic acid vertex at [1, 0].

The residue curves in mole fraction space are shown in Figure 7. The boundaries also correspond to local maxima in the length of the residue curves in mole fraction space (because the curves necessarily lie on a two-dimensional reaction equilibrium surface that is not explicitly shown in the diagrams).

Example 4: Isobutene (1)/Methanol (2)/MTBE (3)/*n*-Butane (4). The system comprising isobutene, methanol, and MTBE (sometimes with *n*-butane) is, perhaps, the most frequently studied reactive system because of the (now somewhat

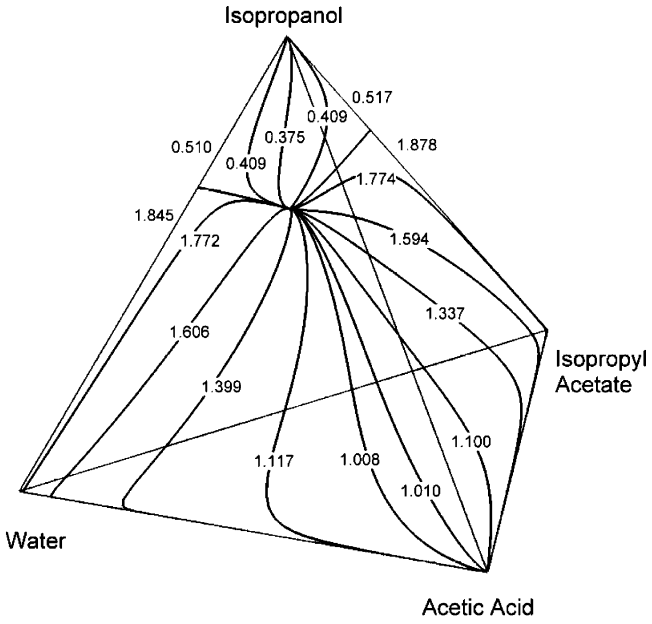

Figure 7. Residue curve map for isopropyl acetate chemistry in mole fraction space. Numbers represent lengths of closest residue curve in mole fraction space.

diminished) commercial significance of MTBE. This is another four-component system, but in this case, one of the components (*n*-butane) is inert; the reaction is

$$\text{isobutene} + \text{methanol} \rightleftarrows \text{MTBE}$$

Vapor−liquid equilibrium in this system was computed using the model described by Ung and Doherty.[17] The liquid phase was modeled using the standard activity coefficient approach. Parameters for the Wilson activity coefficient model and Antoine vapor pressure constants are given by Ung and Doherty.[17]

Since *n*-butane does not take part in the reaction, chemical equilibrium for this case is represented by

$$K_R = \frac{\gamma_3 x_3}{\gamma_1 x_1 \gamma_2 x_2} \tag{21}$$

Following Ung and Doherty,[19] we make MTBE the reference component, and the two independent transformed composition variables are

$$X_1 = \frac{x_1 + x_3}{1 + x_3}; \quad X_2 = \frac{x_2 + x_3}{1 + x_3} \tag{22}$$

This system usually is studied at high pressure (∼8−11 atm) because those are the conditions more likely to be employed in the making of MTBE. We have computed the RCM at 10 and 11 atm, but we begin by showing in Figure 8 the RCM for this system at a pressure of 1 atm. This figure is similar to Figure 1 of Ung and Doherty.[19] The map appears to be split almost precisely in two parts. Curves in the upper half emanate from the binary (nonreactive) azeotrope on the methnol−*n*-butane axis, ending at the methanol vertex. Curves in the lower half of the triangle start at the isobutene vertex and converge at a point halfway up the hypotenuse. Ung and Doherty[19] call the point of convergence a pseudo-azeotrope. This is not a true azeotrope in that the conditions at the point of convergence do not exactly satisfy the stationary point equations (eq 8). It does, however, serve as a severe pinch that acts as a stable node to curves in the lower half of the composition triangle and as a saddle point

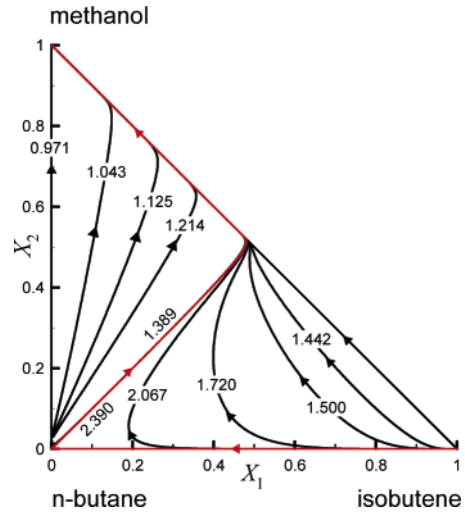

Figure 8. Residue curve map for MTBE system at 1 atm: ● , azeotrope.

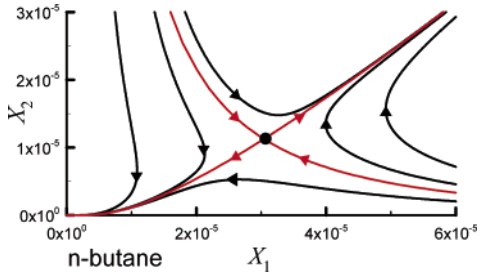

Figure 9. Residue curve map for MTBE system at 1 atm; expanded view near *n*-butane vertex: ● , azeotrope.

to curves in the upper half. In fact, all of the curves in Figure 8 end at the methanol vertex.

The numbers on or adjacent to the various lines in Figure 8 again represent the length of the respective residue curves. We see that the longest of the residue curves in Figure 8 starts at the isobutene vertex, and then follows the isobutene−*n*-butane edge (the *x*-axis) before turning sharply and aiming for the convergence point approximately halfway along the hypotenuse. It then follows the hypotenuse to the methanol vertex. But does this curve represent a boundary in the sense that we mean in this paper: a curve that starts at an unstable node, splits at a saddle point, each branch then ending at a stable node? The *n*-butane vertex would be a most unusual saddle point, given that there appears to be no stable node other than the methanol vertex to which a boundary splitting at the *n*-butane vertex can connect. This suggests that it might be wise to look closer at the *n*-butane vertex and its immediate surroundings.

Figure 9 shows a close-up view of the neighborhood around the *n*-butane vertex. We clearly see the characteristic pattern of residue curves in the vicinity of a saddle-point azeotrope. The closeness of this saddle point to the *n*-butane vertex means that it is extremely easy to miss when constructing a residue curve map for this system. In fact, Ung and Doherty did not find a reactive azeotrope at a pressure of 1 atm (although Ung[16] suspected that one might exist).

The presence of the saddle point explains why the longest residue curve in Figure 8 behaves as it does in the vicinity of the *n*-butane vertex. A saddle-point azeotrope in a system with two degrees of freedom needs four other stationary points to which it can connect. In this case, there are precisely four other stationary points, with no additional stationary points to which the saddle is not connected. These four stationary points are the vertices for methanol, isobutene, and *n*-butane, and the

binary nonreactive methanol−*n*-butane azeotrope. The binary azeotrope and the isobutene vertex are unstable nodes of eq 6, and the methanol and *n*-butane vertices are stable nodes. MTBE cannot exist as a pure component in the presence of reaction. The ideal system considered earlier is another example with a reactive saddle-point azeotrope with precisely four other stationary points to which it connects (the four pure components in that case) and no unconnected stationary points. However, the shapes of the boundary curves in the MTBE system are markedly different from those of the ideal system in Figure 3.

The counterpart to the longest curve described above is from the isobutene vertex to the saddle point, ending at the *n*-butane vertex and creating a distillation region that is an extremely narrow sliver of the composition triangle close to the *n*-butane−isobutene axis. There is also a boundary curve from the nonreactive binary azeotrope on the methanol−*n*-butane axis to the reactive saddle-point azeotrope, to the point of convergence on the hypotenuse, and ending at the methanol vertex. The other side of this boundary curve is from the methanol−*n*-butane binary azeotrope to the saddle point, ending at the *n*-butane vertex. Although this curve is not very long, it is the longest curve in the very tiny distillation region between this residue curve and the methanol−*n*-butane (*y*) axis.

The reactive saddle-point azeotrope exists at all pressures from 0.01 to 11 atm (and in all likelihood exists outside this range—we just did not look any further). The variation of the composition of the reactive azeotrope with pressure is shown in Figure 10. These calculations were carried out with 22-digit arithmetic in order to ensure sufficient accuracy (see Appendix A).

Thus, the structure of the RCM at high pressures is unchanged from that shown in Figures 8 and 9; the only difference is that the pseudo-azeotrope on the hypotenuse opens up slightly and the reactive saddle-point azeotrope moves further inside the triangle.[19]

Kinetically Controlled Reactions

The influence of homogeneous reaction kinetics on chemical phase equilibria and reactive azeotropy were investigated first by Venimadhavan et al.[27] and Rev.[28] For a single reaction, the residue curves are obtained from

$$\frac{dx_i}{d\xi} = x_i - y_i + Da(\nu_i - \nu x_i)\mathscr{R} \tag{23}$$

where ξ is a dimensionless time, the ν_i are the stoichiometric coefficients (with $\nu = \sum_{i=1}^{c}\nu_i$ the overall stoichiometric coefficient), and $\mathscr{R} = r/r_{ref}$ is a dimensionless reaction rate. *Da* is the Damkohler number (a dimensionless measure of the rate of reaction) defined by $Da = Hr_{ref}/V$, where *H* is the molar holdup and *V* is the molar flow of vapor leaving the still (for a derivation, see ref 5 pp 435 et seq.).

When $Da = 0$, eq 23 simplifies to eq 1 for nonreacting systems. The other extreme of high *Da* leads to a reaction equilibrium for which we have eq 6, as discussed in Section 3. For other values of the Damkohler number, eq 23 must be expressed in terms of mole fractions, because for kinetically controlled systems there is no composition transformation that can lead to the simple form of eq 6.

The stationary points of these equations are obtained by setting the derivative terms in eq 23 to zero:

$$Da\mathscr{R} = \frac{x_i - y_i}{\nu_i - \nu x_i} \tag{24}$$

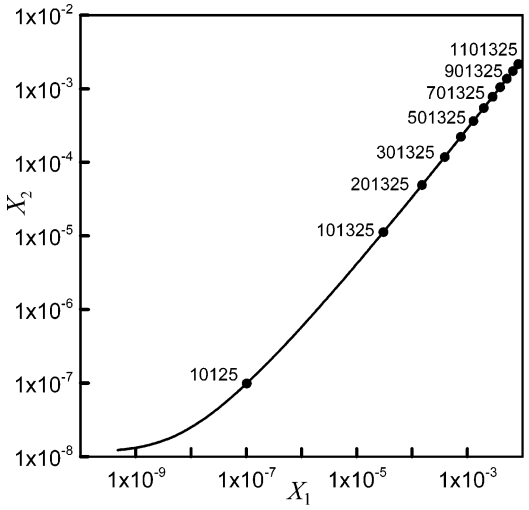

Figure 10. Composition of reactive azeotrope in MTBE system as a function of pressure. Numbers indicate pressure in Pa of azeotrope at nearest point. Pressures at unlabeled points are 1 bar higher or lower than at adjacent points.

Solutions to these equations include some of the pure components (but not all of them in a reacting system), azeotropes that survive the reaction, and any kinetic azeotropes that would exist as a result of reaction. In many—perhaps most—cases in which kinetics controls the reaction, there also exist singular points in nonphysical space (i.e., with negative or complex-valued mole fractions).

It is clear that solutions to eq 23 depend on the Damkohler number, and it should also be clear that *Da* depends on time insofar as the reaction rate, holdup, and vapor flow rate change with time. It is common to assume constant *Da* when integrating eq 23; this is equivalent to assuming that *V* and *H* change at the same rate. An alternative is to assume that *V* is a constant, but this assumption leads to a set of nonautonomous differential equations (because ξ appears on the right-hand side) and more complicated behavior, including residue curves that may cross.[27]

Example 5: The MTBE System One More Time. Consider again the system isobutene (1), methanol (2), and MTBE (3). Earlier, we looked at this system in the absence of reaction; we have also added the inert *n*-butane to the mixture and considered reaction equilibrium. Here, we look at the effects of a kinetically controlled reaction in this system.

The reaction rate is represented by

$$\mathscr{R} = \frac{r}{r_{ref}} = \frac{k_f}{k_{f,min}}\left(x_1\gamma_1 x_2\gamma_2 - \frac{1}{K}x_3\gamma_3\right) \tag{25}$$

with

$$\ln K = 6820/T - 16.33 \tag{26}$$

and $k_{f,min} = 0.0052\ \text{min}^{-1}$. The activity coefficients in eq 25 (and in the VLE equations) are calculated from the Wilson model.

Figure 11 shows the residue curve map for this ternary system at a pressure of 8 atm for $Da = 0.12$. The diagram is essentially the same as Figure 12b of Venimadhavan et al.,[27] with the addition here of the lengths of the various residue curves.

Under the conditions that prevail in this illustration, there are two reactive azeotropes within the borders of the composition triangle, a stable node with respect to eq 23, and a saddle point. It is to be noted that, when reaction kinetics plays a role, the

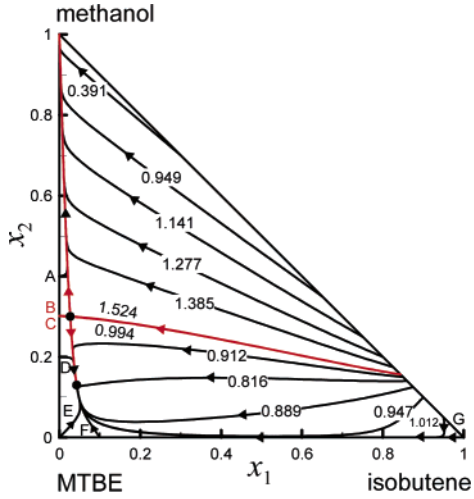

Figure 11. Residue curve map for the MTBE system at 8 atm and for a Damkohler number of 0.12. Numbers represent line lengths: ●, azeotrope. Curves identified by letters have the following lengths: A = 0.607, B = 0.720, C = 0.190, D = 0.091, E = 0.121, F = 0.134, and G = 1.020.

curves do not all start and end at a fixed point in the composition triangle. Were we to integrate backward in ξ, we would find that the curves that pass through the hypotenuse end at an unstable node (with respect to eq 23) that lies outside the composition triangle. The situation is not so simple for the other residue curves in Figure 11. Those that start on the *x*-axis in the vicinity of the MTBE vertex and those that start on the *y*-axis when traced backward appear to simply come to an end, with the numerical integration taking vanishingly small steps. There is no unique end point for these curves. Nevertheless, we find that the curves that mark the edges of the different regions in this map are, once again, those that are longest, provided that we consider only that portion of the curve that lies within or on the borders of the composition triangle. Thus, boundaries in systems with two degrees of freedom are maximum line integrals, even when the curves do not have common end points.

The optimization procedure devised by Lucia and Taylor[1] to find the lines of maximum length needs to be adapted in order to locate the boundaries in these systems where reaction kinetics are important. The reason is that there is no small set of nodes that anchor the ends of each family of residue curves; rather, all points on the edge of the triangle may be valid starting points for a kinetically controlled residue curve, and each composition on the edge of the triangle can be considered to be an end point of a unique residue curve. One possible modification is to adapt the algorithm so that, instead of searching for the angle of departure from a node of known composition, we search instead for the composition(s) along the edge of the triangle that are the starting points for the lines of maximum length. A simpler alternative is to integrate backward from starting points in a ball around the stable node. The integrations would be halted upon encountering infeasible compositions (negative or, much less likely, complex mole fractions).

Heterogeneously Catalyzed Reactions. Residue curve maps and heterogeneous kinetics in methyl acetate synthesis have been measured by Song et al.[29] They find that the residue curves for the kinetically controlled cases are qualitatively similar to the curves for the equilibrium case. Song et al. also provided the first experimental evidence for a reactive azeotrope. More recently, Huang et al.[23] have measured isothermal residue curves and located a reactive azeotrope for a similar reaction system that produces propyl acetate. Figure 8 in their paper shows that the residue curve map is structurally similar to the isopropyl acetate system shown in Figure 5, and it is apparent that the boundaries will be the longest curves for this system also.

Thiel et al. compute the residue curves for the heterogeneously catalyzed reactive distillation of MTBE, TAME (*tert*-amyl methyl ether),[30] and ETBE (ethyl *tert*-butyl ether)[31] and find them to have significantly different shapes versus the homogeneously catalyzed residue curves.[27] They also show the influence of the Damkohler number and the operating pressure on the existence and location of fixed points in the residue curve map. Inspection of Figures 2b and 6 of Thiel et al.[30] shows that the boundary curves again are local maxima in line integrals.

Reactions in Systems with Two Liquid Phases. Okasinski and Doherty[32] extended their own earlier work of 1997 to cover heterogeneous reactive mixtures, thereby enabling the determination of the existence and location of reactive azeotropes in systems with two liquid phases. Qi et al.[33] considered reaction kinetic effects in systems with multiple liquid phases. It is clear from Figures 6 and 8 of their paper that everything we have said about boundaries in systems with two degrees of freedom being maximum line integrals carries over to the heterogeneous case.

Conclusions

In this paper, the geometric characterization of exact separation boundaries recently proposed by Lucia and Taylor[1] was shown to apply to both equilibrium and kinetically controlled reactive separations. This characterization states that separation boundaries correspond to residue curves that are local maxima in line integrals, surface areas, and volumes from any given unstable node to all reachable stable nodes. For equilibrium-governed reactive separations, extension of our geometric theory follows readily from the usual transformations from mole fractions to transformed mole fractions (e.g., eq 5). For kinetically controlled reactive separations, the Damkohler number is an important system parameter, and extension of the original theory requires that integration proceed from feasible stable nodes to a terminus on the boundary of the feasible region since these systems can exhibit stationary points outside the feasible region.

A number of benchmark examples of equilibrium and kinetically controlled reactive separations with two degrees of freedom were studied to illustrate the power of our geometric theory in finding exact separation boundaries. Both ideal and nonideal vapor- and liquid-phase behavior was investigated. In particular, the reactive MTBE separation was studied under conditions of equilibrium and kinetically controlled operation. Other examples studied were an ideal four-component mixture and the production and separation of isopropyl acetate with association in the vapor phase. Numerical results clearly show that separation boundaries for reacting systems with two degrees of freedom correspond to line integrals of maximum length and that the residue curves that define these boundaries occur at one-sided cusp points in the distance function—as predicted by theory. A number of other types of reactive separations (e.g., heterogeneously catalyzed reactive separations and reactive separations with two liquid phases) were also discussed, and it was noted that residue curve maps currently in the open literature for these systems clearly show that the geometric theory of separation boundaries of Lucia and Taylor[1] applies to those cases as well, despite the fact that no line integral values have been computed for these systems. In fact, extension of our geometric theory to these systems seems to be obvious.

Acknowledgment

A.L. would like to thank the National Science Foundation for financial support under Grant No. CTS-0113091.

Appendix A: Computational Details

The computations reported by Lucia and Taylor[1] for nonreacting systems were carried out in compiled Fortran programs. Numerical integration of the residue curve equations was done using Euler's method and/or Runge−Kutta methods. The terrain-following optimization method of Lucia and Yang[34,35] was employed to solve the optimization problem posed by eq 3. Stationary points (pure components and azeotropes) were found using the same optimization method.

All of the computations carried out for this paper were done with the computer algebra system Maple. The differential algebraic equation system for a residue curve was solved using an implementation in Maple of BESIRK, a code that combines Michelsen's third-order SIRK method with a Bulirsch−Stoer extrapolation method (based on a prime number step sequence).[36−38]

For this work, consistent initial points and stationary points were computed using a constrained Newton's method. Mole fractions were prevented from straying outside the valid range from 0 to 1, and temperatures were not allowed to change by more than 10 K per iteration.

There should be no question that the terrain-following method would be equally effective at solving the optimization problem defined by eq 9 for systems in reaction equilibrium. For this work, however, we used the function fdiscont in Maple for finding discontinuities in functions. This procedure works via the application of divided differences. In most cases, it is necessary to increase the precision of the calculations in Maple by using more digits than the default number of 10. This necessarily increases the time needed to obtain a solution, and we do not recommend the use of Maple if the rapid determination of separation boundaries is desired.

We must also describe how the initial points were computed for Example 3, because it is essential to start the integrations from a consistent set of mole fractions, transformed composition variables, and temperature. In an early phase of this investigation, we tried to specify two liquid-phase mole fractions and compute the remaining mole fractions from the reaction equilibrium eq 19. This proved difficult in practice, since it is much too easy to specify a pair of mole fractions that do not lie on the reaction equilibrium surface. A strategy that we found completely successful was to specify the initial values of the transformed composition variables for the liquid phase, X_1 and X_2. The reaction equilibrium eq 19 can be expressed in terms of these two composition variables, one unknown mole fraction, x_3 say, and temperature. This equation may easily be solved for the mole fraction x_3 for an estimated temperature (close to the temperature of the reactive azeotrope). For any specified X_1 and X_2 and computed x_3, it is possible to compute the remaining liquid-phase mole fractions from eq 20 and the mole fraction summation equation. While this equation sometimes has two solutions for x_3 in the range $0 \le x_3 \le 1$, only one of them leads to physically meaningful values for *all* of the other mole fractions. The vapor-phase mole fractions follow from eq 15. The fact that the right-hand sides include the vapor-phase mole fractions poses no difficulties to the computation of the y_i. The transformed compositions for the vapor follow directly. This procedure provides an excellent set of values with which to initialize a simultaneous solution of the chemical and phase-equilibrium equations for a consistent set of mole fractions, transformed compositions, and the equilibrium temperature.

Literature Cited

(1) Lucia, A.; Taylor, R. The Geometry of Separation Boundaries: Basic Theory and Numerical Support. *AIChE J.* **2006**, *52*, 582.

(2) Ostwald, W. Dampfdrucke Ternarer Gemische, Abahndlungen der Mathematisch-Physischen der Konig Sachsischen. *Ges. Wiss.* **1900**, *25*, 413.

(3) Ostwald, W. *Lehrbuk der Allgemetnen Chemie*; Engelmann: Leipzig, Germany, 1902.

(4) Schreinemakers, F. A. H. Dampfdrucke Ternarer Gemische. *Z. Phys. Chem.* **1901**, *36*, 257, 413, 711.

(5) Doherty, M. F.; Malone, M. F. *Conceptual Design of Distillation Systems*; McGraw-Hill: New York, 2001.

(6) Taylor, R.; Krishna, R. Modelling Reactive Distillation. *Chem. Eng. Sci.* **2000**, *55*, 5183−5229.

(7) Pöllmann, P.; Blass, E. Best Products of Homogeneous Azeotropic Distillations. *Gas Sep. Purif.* **1994**, *8*, 194−228.

(8) Fien, G.-J. A. F.; Liu, Y. A. Heuristic Synthesis and Shortcut Design of Separation Processes Using Residue Curve Maps: A Review. *Ind. Eng. Chem. Res.* **1994**, *33*, 2505−2522.

(9) Widagdo, S.; Seider, W. D. Azeotropic Distillation. *AIChE J.* **1996**, *42*, 96.

(10) Kiva, V. N.; Hilmen, E. K.; Skogestad, S. Azeotropic Phase Equilibrium Diagrams: A Survey. *Chem. Eng. Sci.* **2003**, *58*, 1903−1953.

(11) Barbosa, D.; Doherty, M. F. Theory of Phase Diagrams and Azeotropic Conditions for Two-Phase Reactive Systems. *Proc. R. Soc. London, Ser. A* **1987**, *413*, 443−458.

(12) Barbosa, D.; Doherty, M. F. A New Set of Composition Variables for the Representation of Reactive Phase Diagrams. *Proc. R. Soc. London, Ser. A* **1987**, *413*, 459−464.

(13) Barbosa, D.; Doherty, M. F. The Influence of Chemical Reactions on Vapor−Liquid Phase Diagrams. *Chem. Eng. Sci.* **1988**, *43*, 529−540.

(14) Barbosa, D.; Doherty, M. F. The Simple Distillation of Homogeneous Reactive Mixture. *Chem. Eng. Sci.* **1988**, *43*, 541−550.

(15) Doherty, M. F. Topological Theory of Phase Diagrams for Reacting Mixtures. *Proc. R. Soc. London, Ser. A* **1990**, *430*, 669−678.

(16) Ung, S. Distillation of Mixtures with Multiple Chemical Reactions. Ph.D. Thesis, University of Massachusetts, Amherst, MA, 1994.

(17) Ung, S.; Doherty, M. F. Vapor−Liquid-Phase Equilibrium in Systems with Multiple Chemical Reactions. *Chem. Eng. Sci.* **1995**, *50*, 23−48.

(18) Ung, S.; Doherty, M. F. Theory of Phase Equilibria in Multireaction Systems. *Chem. Eng. Sci.* **1995**, *50*, 3201−3216.

(19) Ung, S.; Doherty, M. F. Calculation of Residue Curve Maps for Mixtures with Multiple Equilibrium Chemical Reactions. *Ind. Eng. Chem. Res.* **1995**, *34*, 3195−3202.

(20) Ung, S.; Doherty, M. F. Necessary and Sufficient Conditions for Reactive Azeotropes in Multireaction Mixtures. *AIChE J.* **1995**, *41*, 2383−2392.

(21) Rowlinson, J. S. *Liquids and Liquid Mixtures*, 2nd ed.; Butterworth: London, 1969.

(22) Song, W.; Huss, R. S.; Doherty, M. F.; Malone, M. F. Discovery of a Reactive Azeotrope. *Nature* **1997**, *388*, 561−563.

(23) Huang, Y.-S.; Sundmacher, K.; Tulashie, S.; Schlünder, E.-U. Theoretical and Experimental Study on Residue Curves Maps of Propyl Acetate Synthesis Reaction. *Chem. Eng. Sci.* **2005**, *60*, 3363−3371.

(24) Okasinski, M. J.; Doherty, M. F. Thermodynamic Behavior of Reactive Azeotropes. *AIChE J.* **1997**, *43*, 2227−2238.

(25) Maier, R. W.; Brennecke, J. F.; Stadtherr, M. A. Reliable Computation of Reactive Azeotropes. *Comput. Chem. Eng.* **2000**, *24*, 1851−1858.

(26) Venimadhavan, G.; Malone, M. F.; Doherty, M. F. Bifurcation Study of Kinetic Effects in Reactive Distillation. *AIChE J.* **1999**, *45*, 546−556.

(27) Venimadhavan, G.; Buzad, G.; Doherty, M. F.; Malone, M. F. Effect of Kinetics on Residue Curve Maps for Reactive Distillation. *AIChE J.* **1994**, *40*, 1814−1824.

(28) Rev, E. Reactive Distillation and Kinetic Azeotropy. *Ind. Eng. Chem. Res.* **1994**, *33*, 2147−2179.

(29) Song, W.; Venimadhavan, G.; Manning, J. M.; Malone, M. F.; Doherty, M. F. Measurement of Residue Curve Maps Heterogeneous Kinetics in Methyl Acetate Synthesis. *Ind. Eng. Chem. Res.* **1998**, *37*, 1917−1928.

(30) Thiel, C.; Sundmacher, K.; Hoffmann, U. Residue Curve Maps for Heterogeneously Catalysed Reactive Distillation of Fuel Ethers MTBE and TAME. *Chem. Eng. Sci.* **1997**, *52*, 993−1005.

(31) Thiel, C.; Sundmacher, K.; Hoffmann, U. Synthesis of ETBE: Residue Curve Maps for the Heterogeneously Catalysed Reactive Distillation Process. *Chem. Eng. J.* **1997**, *66*, 181−191.

(32) Okasinski, M. J.; Doherty, M. F. Prediction of Heterogeneous Reactive Azeotropes in Esterification Systems. *Chem. Eng. Sci.* **2000**, *55*, 5263−5271.

(33) Qi, Z.; Kolah, A.; Sundmacher, K. Residue Curve Maps for Reactive Distillation Systems with Liquid-Phase Splitting. *Chem. Eng. Sci.* **2002**, *57*, 163−178.

(34) Lucia, A.; Yang, F. Global Terrain Methods. *Comput. Chem. Eng.* **2002**, *26*, 529−546.

(35) Lucia, A.; Yang, F. Multivariable Terrain Methods. *AIChE J.* **2003**, *49*, 2553−2563.

(36) Kooijman, H. A. Dynamic Nonequilibrium Column Simulation. Ph.D. Thesis, Clarkson University, Potsdam, NY, 1995.

(37) Kooijman, H. A.; Taylor, R. A Dynamic Nonequilibrium Model of Tray Distillation Columns. *AIChE J.* **1995**, *41*, 1851−1863.

(38) Schwalbe, D.; Kooijman, H. A.; Taylor, R. Solving Stiff Differential Equations and Differential Algebraic Systems with Maple V. *Maple Technol. J.* **1996**, *3*, 47−53.

Received for review July 26, 2005
Revised manuscript received February 7, 2006
Accepted February 15, 2006

IE0508740